Biomechan Model Mechanobiol (2005) 4: 1–9
DOI 10.1007/s10237-004-0061-8

ORIGINAL PAPER

Liang Zhu · Liewen Pang · Lisa X. Xu

Simultaneous measurements of local tissue temperature and blood perfusion rate in the canine prostate during radio frequency thermal therapy

Received: 15 July 2004 / Accepted: 23 November 2004 / Published online: 7 June 2005

Abstract Local tissue temperature and blood perfusion rate were measured simultaneously to study thermoregulation in the canine prostate during transurethral radio-frequency (RF) thermal therapy. Thermistor bead microprobes measured interstitial temperatures and a thermal clearance method measured the prostatic blood perfusion rate under both normal and hyperthermic conditions. Increase in local tissue temperature induced by the RF heating increased blood perfusion throughout the entirety of most prostates. The onset of the initial increase in blood perfusion was sometimes triggered by a temporal temperature gradient at low tissue temperatures. When tissue temperature was higher than 41°C, however, the magnitude and the spatial gradient of temperature may play significant roles. It was found that the temperature elevation in response to the RF heating was closely coupled with local blood flow. The resulting decrease in or stabilization of tissue temperature suggested that blood flow might act as a negative feedback of tissue temperature in a closed control system. Results from this experiment provide insights into the regulation of local perfusion under hyperthermia. The information is important for accurate predictions of temperature during transurethral RF thermal therapy.

L. Zhu (✉)
Department of Mechanical Engineering,
University of Maryland Baltimore County,
1000 Hilltop Circle, Baltimore, 21250, MD, USA
Tel.: +1-410-4553332
Fax: +1-410-4551052

L. Pang
Shanghai Huashan Hospital, Shanghai,
Peoples Republic of China

L. X. Xu
Department of Mechanical Engineering, Purdue University,
West Lafayette, 47907, IL, USA

1 Introduction

Benign prostatic hyperplasia (BPH) is a disease that affects the quality of life of most aged men. It is often associated with neoplastic lesions in the form of spheroids or nodules that grow within the gland. As an alternative to the traditional surgical treatment, localized microwave or RF thermal therapy was under intensive studies (Baert et al. 1992; Homma and Aso 1993; Larson et al. 1996; Marteinsson and Due 1994; Mulvin et al. 1994; Nissenkorn and Meshorer 1993; Rossette et al. 1993; Sapozink et al. 1993). Utilization of transurethral microwave and RF applicator can assure easy and accurate placement within the prostatic urethra. This allows heat to be deposited preferentially in the immediate peri-urethral tissue region. The interstitial temperature can be elevated up to 60°C to induce coagulation of the abnormal peri-urethral tissue growth that causes urinary obstruction. The likelihood of success of treatment is related to the administration of an optimal thermal dose to overcome the convective effect of blood flow. Previous experimental and theoretical studies showed that local blood perfusion has its profound effect on the temperature distribution during therapy (Martin et al. 1992; Xu et al. 1998a). To maximize the efficiency and safety of the treatment, it is important to study the response of blood perfusion to heating and how it affects the elevation of tissue temperature.

As is well known, local heating may cause blood perfusion to increase above its baseline value, which is generally attributed to a thermally induced local vasodilation. The perfusion increase, if sufficient, can decrease the tissue temperature. Different kinds of temperature responses to local heating in both normal and tumor tissues were observed and discussed by many investigators (Devonec et al. 1993; Larson and Collins 1988; Ranade et al. 1995; Roemer et al 1985, Sekins et al 1984, Song 1984; Xu et al. 1998a, 1998b; Zhu et al. 1995). Those responses include (1) tissue temperature rises monotonically with time to an elevated steady-state

value; (2) temperature rises above a "critical temperature" before an abrupt increase in blood perfusion that decreases the temperature to a new steady-state value; (3) temperature responds as damped oscillations; and (4) temperature responds as self-sustained large oscillation. The first two responses were explained as being induced due to increase in local blood perfusion rate. In the Pennes bioheat transfer equation (Pennes 1948), the blood effect is described as a heat sink and is given by

$$\rho c \frac{\partial T_t}{\partial t} = k_t \nabla^2 T_t + \rho c \omega (T_a - T_t) + q_m + q_{ext} \quad (1)$$

where k_t is thermal conductivity of tissue, ρ is blood density, c is specific heat of blood, ω is local blood perfusion rate, q_m is local metabolic heat generation rate, and q_{ext} is volumetric heat generation rate by external devices. T_a is arterial temperature and is usually 37°C. The transient temperature rate $\partial T_t/\partial t$ changing from a positive to a negative value is determined by the combined effects of heat conduction, a heat sink (blood flow), and a heat source term (RF heating, metabolism, etc.). Once the increase in blood perfusion is large enough to overcome the effects of the heat source and heat conduction, tissue temperature would decrease despite the external heating.

To model oscillatory responses, a non-linear component has to be introduced to the linear Pennes equation. The causes for the oscillatory responses are not obvious since there was no simultaneous measurement of the local temperature and blood perfusion rate during the transient processes of hyperthermia. No direct experimental observation had been performed to reveal the coupled relationship between tissue temperature and local blood flow with respect to the heating time. Such an observation would provide insight into how blood flow regulates tissue temperature resulting in different temperature responses to diathermy.

Several theoretical studies (Losev 1993; Tharp and Zhang 1993) were proposed to explain the temperature oscillations observed experimentally. Tharp and Zhang (1993) postulated that the blood perfusion term was related directly to change of tissue temperature with a time delay. It was shown that under certain conditions, the oscillatory temperatures would occur if the time delay is long enough. Losev (1993) also suggested that undamped temperature oscillations are possible if the blood perfusion term is assumed as a function of previous values of local temperature. A recent theoretical study by Chen and Xu (2002) showed that no oscillation could take place without any time delay in the change of local flow in response to the elevation of tissue temperature. The minimal value of the time delay was predicted by the theory to vary between 3 s and 240 s. It is possible that the local temperature gradient and heating rate are the main factors that determine the minimal time delay. Although the previous theoretical studies provided insight into the possible vascular thermoregulation, no in vivo experimental study has been performed to verify the hypothesis proposed by the theory.

In the present research, a thermal clearance method was used to measure simultaneously the temperatures of canine prostatic tissue and blood flow at the same tissue location. Specifically, experiments were designed to examine: (1) the magnitudes of the blood flow increase shortly after the power is increased; (2) the relationship between temperature and blood flow after the onset of heat-induced hyperemia; (3) whether there exists a threshold temperature above which an abrupt increase in blood flow would occur in the canine prostate; and (4) whether the increase in blood flow is also associated with the temporal gradient of tissue temperature. Results from this study are expected to provide more realistic information for developing a thermoregulation model in the prostate during hyperthermia treatment for BPH.

2 The RF heating apparatus

The EESY-100 Radio Frequency Prostatic Hyperthermia System (Yuanshui Industrial Company, Shanghai, China) was used in this study. This system consists of a RF generator operating at 200 kHz with the maximum of 80 W, a multi-channel thermocouple thermometry system, an IBM computer with special peripherals, and software for monitoring and controlling data acquisition and power output. A continuous, unmodulated sinusoidal output is delivered to two coaxial helical coils wrapping around a 12 G Foley catheter of approximately 6 mm in diameter. The coils are 20 mm apart and connected to the power supply in the control unit. During the experiment, the catheter is inserted into the prostatic urethra to allow good contact between the coil and the prostatic tissue. The tissue is heated by combined current and radiative heating. A thermocouple located inside the catheter monitors the temperature of the urethral wall during the treatment. The power level can be set manually or adjusted through the temperature feedback to maintain the urethral temperature at a certain level during the treatment period.

The specific absorption rate (SAR) distribution induced by the RF catheter was determined in Zhu and Xu (1999) by fitting the transient temperatures at various locations made in a tissue equivalent RF gel phantom. Figure 1 shows the 2-D SAR distribution. The results indicate a rapid fall-off in both the radial and axial direction; in particular, 99% of the RF energy is absorbed in the near region ($r < 15$ mm and $z < 23$ mm). The maximum temperature and temperature gradient of the tissue are expected to be located in the tissue region near the urethra since there is no cooling inside the RF applicator.

3 Theoretical basis of the thermal clearance method

The blood perfusion rate and tissue thermal conductivity were measured simultaneously in the canine prostate using the thermal clearance method, as given in Xu et al.

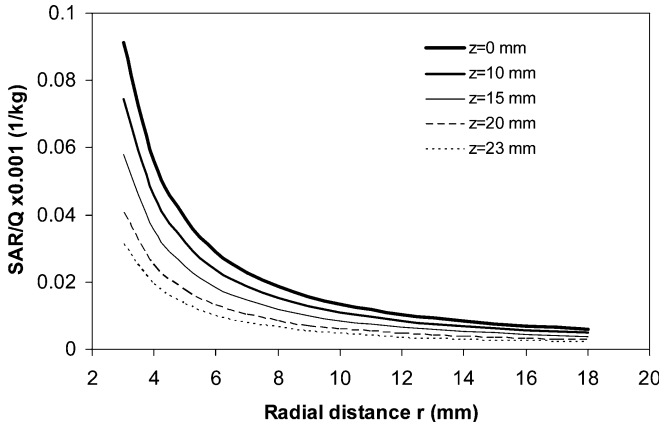

Fig. 1 Specific absorption rate distributions in the radial direction (r) at different axial planes (z). Q is the heating level (W). Note that the two-dimensional SAR is independent of the angle θ in the cylindrical coordinates. The SAR decays in both the radial and axial direction. $z = 0$ represents the axial location when the SAR reaches its maximum

(1998b). Briefly, the technique is based on a comparison of the measured with the model simulated temperature decay following a short heating pulse delivered by a thermzistor bead probe. Based on a given power strength and duration of the pulse, and intrinsic thermal properties for non-perfused tissue, the transient temperature decay is predicted using the Pennes model by adjusting the blood perfusion rate to fit the measurements. The value, which minimized the least square of deviations between the predictions and measurements, is the best estimation of the regional average perfusion rate.

Typically, the Pennes bioheat transfer equation is used to predict the temperature transient. It is assumed that the thermistor bead is a point source inserted into the center of an infinitively large medium. The governing equation and initial condition for this thermal process are described as:

$$\rho c \frac{\partial \theta}{\partial t} = k \frac{1}{r^2} \frac{\partial}{\partial r} \left(r^2 \frac{\partial \theta}{\partial r} \right) + \rho c \omega \theta + q_{\mathrm{p}} \quad t = 0, \;\; \theta = 0 \tag{2}$$

where θ is the temperature elevation after the pulse heating from the pre-heating value, q_{p} is the pulse heating deposited locally into the tissue through a very small thermistor bead probe as: $t_{\mathrm{p}} = P\ \delta(0)$ for $t \leq t_{\mathrm{p}}$ and $t_{\mathrm{p}} = 0$ for $t > t_{\mathrm{p}}$. P is the deposited power, and δ(0) is the Dirac delta function. For the limiting case of an infinitesimally small probe with an infinitesimally short heating pulse, the solution for the above equation for the interval of temperature decay takes the form:

$$\theta = \lambda_2 \int_0^{t_{\mathrm{p}}} (t-s)^{-1.5} \mathrm{e}^{-\omega(t-s)} \mathrm{e}^{-r^2/[(r\lambda_2(t-s)]} \mathrm{d}s \tag{3}$$

where s is the integrated variable, $\lambda_1 = P(\rho c)^{0.5} / (8\pi^{1.5})$ and $\lambda_2 = \alpha \Big/ k_{\mathrm{t}}^{1.5} t_{\mathrm{p}}^{0.5}$. In the theoretical analysis, there are two unknowns, k_t and T. Least square residual fit allows one to find a set of values of k_t and ω, which will lead to the best fit of the theoretical predictions to the experimentally measured temperature decay.

4 Experimental methods

Experimental protocol was reviewed and approved by the local IACUC. Eight male mongrel dogs, weighing 11.1 ± 3.2 kg were anesthetized using Na-pentobarbital, i.v. (30 mg/kg). The bladder and prostate were exposed through a mid-ventral abdominal incision. A small cut was made in the bladder wall to insert the RF catheter into the prostatic urethra. Figure 2 gives a simplified schematic diagram of the vasculature of the prostate and the locations of temperature probes. The typical size of a canine prostate is around 2.1 cm in diameter and 2.5-cm long in the direction of prostatic urethra. The maximum tissue temperature, located at the prostatic urethral wall, was continuously monitored via a thermocouple sensor built inside the RF catheter. Two-to-six thermistor bead probes of different lengths were placed randomly within the prostatic tissue at various radial distances from the catheter wall ($r = 2$–11.5 mm), as shown in Fig. 2. These probes served two purposes: thermal pulse delivery and local temperature measurement. The number of thermistor bead probes used in each dog was limited by the small size of the prostate. Further, the probes were located far enough (at least 5 mm apart) from each other to avoid thermal interactions during the pulse heating. The abdominal incision was then closed and covered with plastic wrap to avoid evaporative cooling from the viscera.

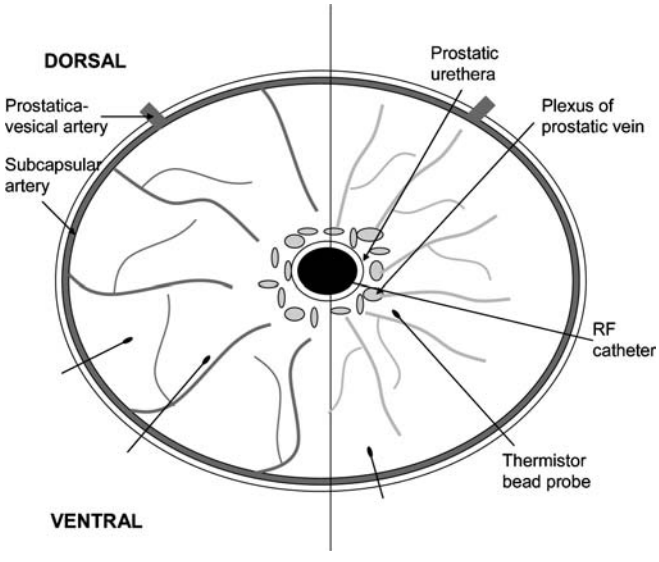

Fig. 2 A simplified schematic diagram of the cross-sectional plane of the canine prostate. The *right side* gives the veins and its branches and the *left side* represents the arteries. The RF catheter is inserted into the prostatic urethra. Several thermistor bead probes are inserted into the tissue from the ventral side of the prostate

In each experiment, the baseline blood perfusion was measured ten times prior to the RF heating. The tissue was then heated for 30 min at the 5 W level during which the interstitial temperatures were measured every second while the urethral temperature was recorded every minute before the power was increased further. At this power level, local blood perfusions at various prostatic locations were measured with an interval of about 3 min. During each measurement, a heating pulse (3 s) was delivered to induce a small thermal disturbance in the local tissue temperature and the subsequent temperature decay was measured for 10 s. The increase in tissue temperature could be contributed by both the RF heating and the pulse heating. The temperature increase due to the RF heating was approximately linear during the short measuring period and can be eliminated from the transient temperature elevation in the computational algorithm. The power was then increased to 10 W, then 15 W, and finally 20 W, each for 30 min. A similar measurement was performed at each power level. At the end of the experiment, and while still under anesthesia, the dog was euthanized by injection of a commercial barbiturate solution (Sleepaway; Fort Dodge Laboratories, Inc. Fort Dodge, IA, USA).

The average blood perfusion rate and thermal conductivity of the tissue are shown as mean ± SD. Differences among the mean values were determined by one-way repeated measures ANOVA using SYSTAT software. The post hoc comparisons between baseline measurement and other heating level were performed by Dunnett's method (Wallenstein 1980). Significance was evaluated at the 5% confidence level.

5 Results

A two-parameter residual fit was performed for the baseline blood perfusion and thermal conductivity measurement at different probe locations within all eight prostates. An average value of $k_t = 0.49 \pm 0.02$ W/m °C ($n = 33$) was obtained for the thermal conductivity of the tissue. Using this average value, one parameter fit was applied to obtain the blood perfusion rates. Figure 3 shows the average perfusion measurements in all prostates after the tissue temperatures reached the steady state at different power levels. For each prostate, the measured blood perfusion rates were averaged over both time and space at each power level. The baseline perfusion rate was found to be 0.68 ± 0.25 ml/min/gm ($n = 8$). Compared to the baseline, even though the average perfusion increased approximately 50% at the 5 W heating level, no statistically significant increase in the perfusion was found. On the other hand, at the 10, 15 and 20 W level significant 1.9-fold, 2.2-fold and 2.5-fold increases in blood perfusion were observed, respectively.

Local RF heating increased the temperatures in the prostatic tissue and urethral wall. Unlike a previously used microwave catheter that has a cooling system to protect the urethral wall (Xu et al. 1998a), the maximum temperature occurs at the prostatic urethral wall with RF heating. As shown in Fig. 4, at the baseline, the average steady-state interstitial temperature (36.3 ± 0.5°C) of all probe locations ($n = 30$) is very close to the average temperature of the urethral wall (36.6 ± 0.6°C) of all prostates ($n = 8$). After the RF power was turned on, a local temperature gradient was established within the canine prostate. The average interstitial temperatures of all canine prostates at the 5, 10, and 15 W were found to be 37.0 ± 0.8°C, 39.4 ± 1.3°C, and 40.7 ± 1.4°C, respectively. The maximum temperatures reached at the urethral wall were 38.2 ± 0.9°C, 42.6 ± 1.4°C, and 46.7 ± 1.8°C, respectively.

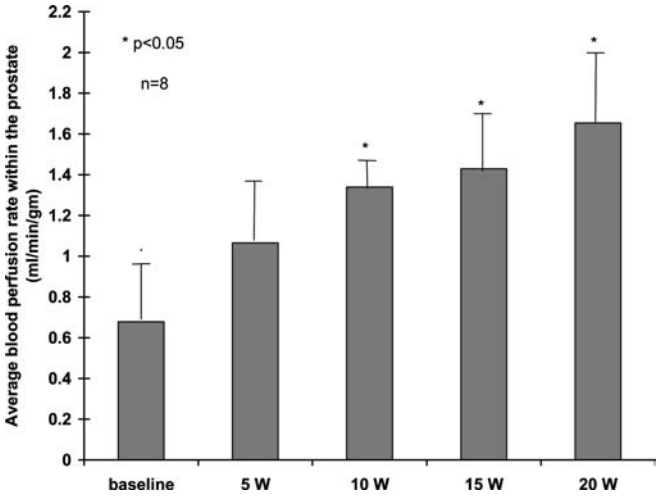

Fig. 3 Average blood perfusion rates in the canine prostates at each heating level during transurethral RF heating. *n* is the number of prostates used in the experiment. *Vertical bar* denotes mean ± SD. *Asterisk* denotes a blood perfusion rate that is significantly different ($p < 0.05$) from that at the baseline

While Figs. 3 and 4 have shown the average values of the blood perfusion rate and tissue temperature in all prostates, Fig. 5 focuses on the large variation of blood perfusion increase and temperature rise among prostates. Different symbols represent different heating levels. Figure 5 suggests a large variation in blood perfusion among prostates. At the 5 W heating level, increase in blood perfusion over the baseline varies between 0 ml/min/gm and 0.7 ml/min/gm. Interstitial temperatures were elevated slightly up to 1°C at this heating level. However, a large increase in blood perfusion may not always be accompanied by a large rise in temperature. When the heating level is elevated (10 W and 15 W), one observes a simultaneous increases in blood perfusion rate and tissue temperature. At the 20 W heating level, the increase in tissue temperature is similar to or slightly higher than that at the 15 W heating level. It suggests that the temperature rise by the increase in the heating (from 15 W to 20 W) may be counterbalanced by the temperature decrease due to the further increase in blood perfusion rate observed at the 20 W heating level.

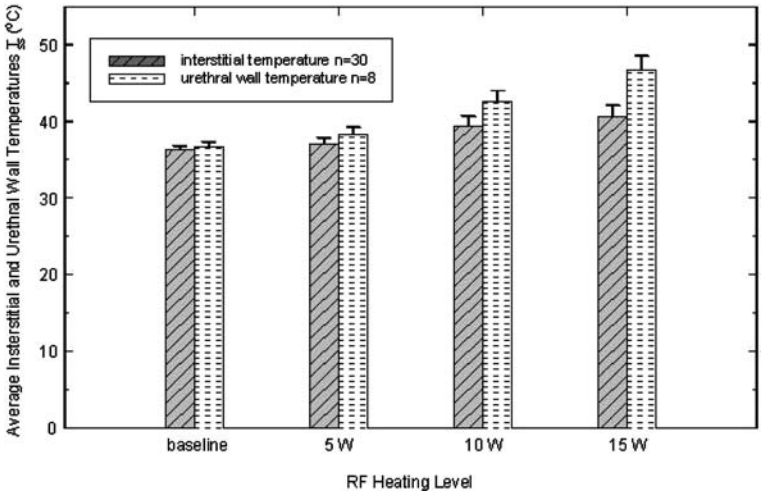

Fig. 4 Interstitial temperatures and urethral wall temperatures measured after the steady state is reached at each heating level. *n* is the total number of measurements by different temperature sensors in eight canine prostates

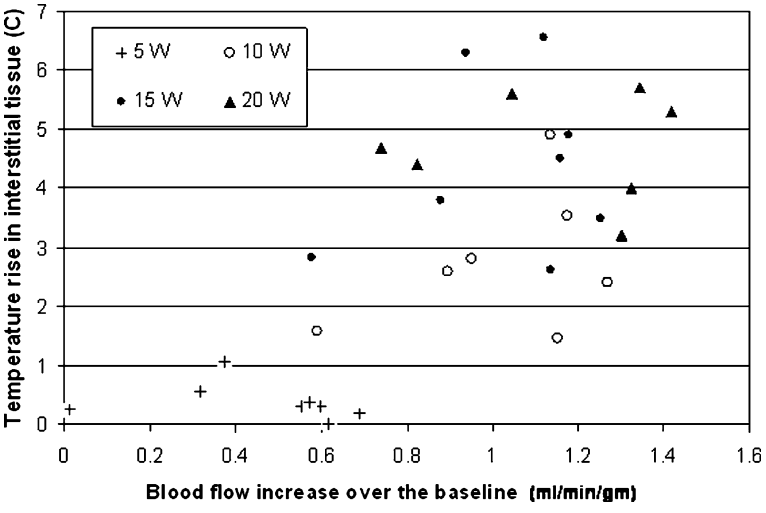

Fig. 5 Relationship between the rise of the interstitial temperatures and the increase in the average blood perfusion rate from the baseline in each prostate. *Different symbols* represent different heating levels. Each symbol gives the average values of the temperatures and blood perfusion rates of each prostate at a specific heating level

During the RF heating, interstitial temperatures were elevated and spatial temperature gradients were established. It is well known that heating can trigger an increase in local blood perfusion rate, which if large enough, can decrease the tissue temperature. Thus, the magnitude of the temperature drop can be viewed as an indication of a large increase in local blood perfusion rate. Figure 6 depicts the relationship between the critical temperature T_{crit}, at which tissue temperature started to decrease and the magnitude of the temperature drop T_{drop} after T_{crit}. One notes a correlation between T_{crit} and T_{drop} within the prostate (open circle) and at the urethral wall (triangle). There existed no clear "threshold" temperature above which large blood flow increase would result in the temperature drop. Large decreases in temperature up to 1.9°C were observed even when the tissue temperatures were relatively low (< 39°C). This indicates that local tissue temperature may not be the sole player in triggering the increase in blood perfusion. During the first several minutes of heating at each power level, tissue temperature started increasing at different rates ranging from 0.5∼2°C/min. The large temporal temperature gradient at the beginning of the lower power level may be the major factor in triggering the blood perfusion increase. At a higher heating level (> 10 W), prostatic temperature was significantly elevated. It was observed that the magnitude of the temperature drop increases with the local temperature. Considering that high tissue temperatures coexisted with large spatial temperature gradients in this study, it seems that when the tissue temperature is higher than 41°C, both the local tissue temperature and spatial temperature gradient become more and more important in determining the magnitude of the increase in blood perfusion.

Figure 7 shows temperature transients measured at the urethral wall (heavy dash line) and at three probe locations inside the prostate (solid lines) during the RF heating. The probes were located at a radial distance of 2, 6 and 7 mm, respectively, from the urethral wall. The largest interstitial temperature rise occurs at the radius location of $r = 2$ mm. Note a similar temperature elevation pattern in the interstitial temperatures and the temperature at the urethral wall, except that the

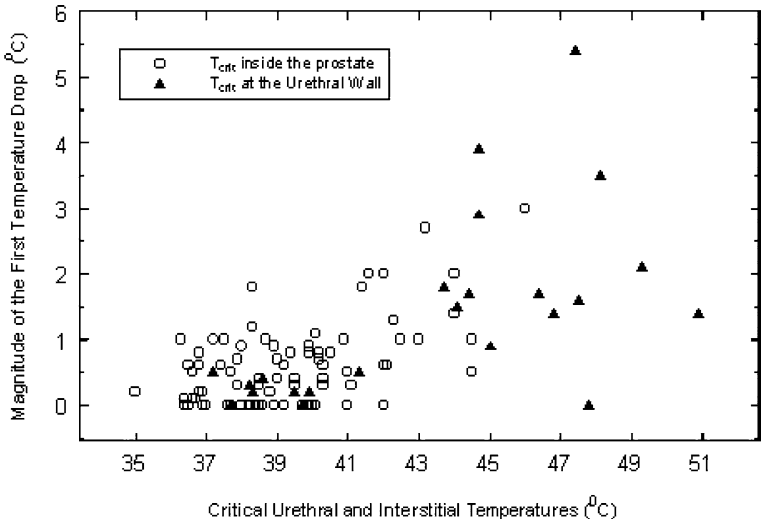

Fig. 6 First temperature drop ΔT_{drop} observed with respect to the critical interstitial temperature and critical urethral wall temperature, T_{crit}

temperature elevation was more moderate inside the prostate. The magnitude of the prostate temperature distribution induced by this kind of RF catheter usually declines progressively with increasing radial distance from the urethral wall, reflecting an exponential decay of the RF energy with the distance from its source (Zhu and Xu 1999). It is suggested that the increase in the local blood perfusion was triggered almost everywhere in this prostate so that similar temperature transient profiles were observed at different measuring sites. The same trend was observed in six out of the eight canine prostates studied. Figure 8 demonstrates a different pattern of temperature elevation observed in the other two of the eight canine prostates. The temperature probes inside the prostate were located at a radial distance of 4 mm to 8 mm from the urethral wall. During the 10 W and 15 W heating levels, the interstitial temperature kept increasing, while the blood perfusion rate was triggered to increase with the tissue temperature. Temperature drop was not observed in all interstitial locations. At the urethral wall, an initial temperature drop was evident at higher heating levels (>10 W). However, the increase in perfusion during the rest of each session might not be big enough to induce an oscillatory temperature response as shown in Fig. 7.

Figure 7 also illustrates simultaneous measurements of tissue temperature and local blood perfusion rates (symbols) during the heating. The perfusion profile has a similar shape as that of the interstitial temperatures, which clearly demonstrates a close relationship between them. As shown in Fig. 7, an increase in perfusion was observed at the beginning of the heating and it kept increasing almost linearly with the local tissue temperature. In Fig. 7, at the 10 W heating level, the blood perfusion increased with the tissue temperature until it reached its maximum of approximately 3 ml/min/gm. Then it started to decrease with the tissue temperature. Once the temperature became more stable after the tissue was heated for about 15 min, the perfusion increased again until a relatively constant value of approximately 1.5 ml/min/gm was reached, which is consistent with the average blood perfusion measurement at the 10 W heating level under the steady state condition. A similar periodic change in perfusion occurred at the 15 W

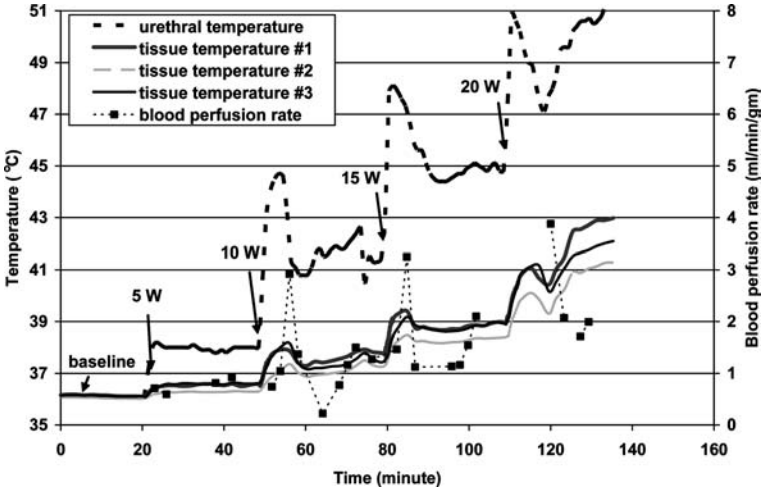

Fig. 7 Blood perfusion rate of a canine prostate measured at different time instants and transient temperature profiles during the RF thermal therapy at four measurement sites (one is at the urethral wall and the other three are inside the canine prostate). The three thermistor beads are located 2, 6, and 7 mm, respectively, from the RF catheter surface

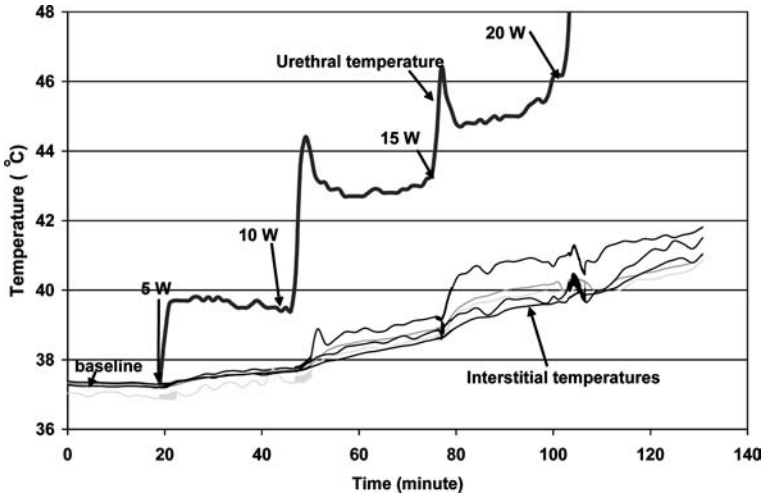

Fig. 8 Different transient profiles between the urethral temperature and interstitial temperature in a prostate

heating level except that it stabilized at a higher level according to the trend. Another interesting phenomena observed in Fig. 7 is that the maximal perfusion and interstitial temperature occurred almost at the same moment, which was several minutes behind the time when the maximal temperature of the urethral wall was reached.

6 Discussion

The normal adult prostate consists of approximately 50% stroma, 30% acinar lumens and 20% epithelium. The two dominant cell types in the glandular tissue of prostate are smooth muscle cells and fibroblasts. Note that the current study was performed on normal canine prostate. The major morphological change in human prostate with BPH is the proliferation of stromal cells with the peri-urethral tissues, while in dogs, both hypertrophy and hyperplasia occur. At this stage, we are not sure how BHP may change the temperature and blood-flow responses to RF heating. However, it is likely that the resulted temperature in the normal canine prostates would be similar to that in prostates with BPH. Temperature elevation can be affected by the thermal conductivity of tissue. Since BPH is characterized by proliferation of the stromal and glandular-epithelial compartments, we don't expect a significant change of thermal conductivity from normal prostatic tissue.

It is widely known that the local perfusion increase, if sufficient, will result in a tissue temperature drop. This can be shown from the Pennes equation, which was used to describe blood flow effects on the tissue temperature (T_t) field. In our experiments, an increase in blood perfusion was observed at almost all measuring sites either directly from the blood perfusion measurement or indirectly from the decrease in local tissue temperature, although the magnitude of the increase varies (Xu et al. 1998b). It was observed that most of the urethral and the interstitial tissue temperature profiles followed the same changing pattern during the RF heating. Thus, the blood flow increase was not a local phenomenon for most of the canine prostates used in this study.

Several factors can affect the trigger of perfusion increase and its magnitude. In Sekins et al. (1984), it was shown that there existed a "threshold temperature" of approximately 42°C above which large flow increase occurred. However, from the present study in the canine prostate during RF thermotherapy, it seems that high tissue temperature is not the sole factor responsible for the blood perfusion increase, since it could occur at a temperature as low as 38°C. This can be interpreted as a much lower threshold temperature in prostate tissue during the RF heating. However, it is also possible that no threshold exists and other factors, such as the rate of temperature rise could play an important role in triggering the increase in local blood perfusion. When tissue temperature was higher than 41°C, the effect of tissue temperature on the increase in perfusion rate became more evident since the magnitude of temperature drop increased with the tissue temperature. It is possible that the rate of temperature rise in tissue determines the magnitude of the increase in local blood perfusion.

When the heating is prolonged, the spatial temperature gradient is also expected to affect blood flow. Local temperature gradient in the prostate tissue cannot be directly derived from the current experiment due to the limited numbers of the thermistor bead probes inserted into the tissue. A previous study by the authors (Zhu and Xu 1999) developed an empirical equation for the tissue-temperature rise during the RF heating. This equation, based on the simulated results for the same RF apparatus as the current study, is given by

$$\Delta T_t(r,z) = QK e^{-(r-3)/r_d} e^{-z^2/z_d^2}$$
$$K = 0.7175\omega^{-0.7237} \quad r_d = 9.4637\omega^{-0.2764}$$
$$z_d = 21.2766\omega^{-0.1746} \tag{4}$$

where ΔT_t is the temperature elevation and Q is the heating level (W). The local temperature gradients can then be derived as

$$\frac{\partial T_t}{\partial r} = -\frac{QK}{r_d} e^{-(r-3)/r_d} e^{-z^2/z_d^2}$$
$$\frac{\partial T_t}{\partial z} = -\frac{QK}{z_d^2} e^{-(r-3)/r_d} e^{-z^2/z_d^2} \quad (5)$$

Obviously, the largest temperature gradient occurs at the catheter surface. Both temperature rise and temperature gradient are proportional to the heating level Q. However, it is hard to distinguish the individual effects of tissue temperature and temperature gradient. In the future, a controlled experiment to separate the temperature rise from temperature gradient is needed to address this issue.

Four kinds of temperature responses, including both damped and sustained oscillation, were previously observed by Roemer et al. (1985) and Xu et al. (1998a). Based on the Pennes bioheat equation, it was suggested that either a second order self-regulatory system had been turned on when local temperature was raised to a certain level or there was a time lag of the local blood perfusion responding to tissue temperature. In this experiment, the simultaneous measurement of blood perfusion rate and local tissue temperature provides us a better understanding of the thermoregulatory behavior in the canine prostate. Once the increase in blood perfusion was triggered, the change in perfusion appeared to be closely related not only to the tissue temperature but also to the temperature gradients. The oscillatory temperature behavior seemed to be coupled with an oscillatory change in blood perfusion. The previous theoretical hypothesis (Chen and Xu 2002) that it is the time delay that results in the oscillatory behavior is observed in the current animal study. The maximal perfusion and interstitial temperature were found to be several minutes behind the time when the maximal urethral wall temperature was reached. Since both the urethral wall and interstitial temperatures are regulated by the blood perfusion that can be viewed as a feedback of local tissue temperature in a closed control system with different time delays, it is not difficult to see why the former is more oscillatory than the latter.

Although the details of the physiological and biochemical bases for the blood response are not fully known, the thermoregulatory controlling factors which influence the blood-flow response to heating are thought to be mainly limited to local effects and not to nonthermal effects. The increase in blood flow is attributed to dilation of arterioles beyond their basal level induced by local extrinsic stimulation. It was shown that temperature and/or temporal temperature gradient can affect the intracellular pathways leading to changes in the state of the contractile proteins of the vascular smooth muscle (Vanhoutte 1980). Such temperature-induced intracellular changes include alteration in cell-membrane potential, Ca^{2+} ion channel conductance, and intracellular enzymatic activity. They can also affect the extracellular chemical substances to initiate vascular smooth muscle contraction and dilation by binding to smooth muscle adrenergic and other membrane receptors or diffusing into the cell to activate intracellular responses (Faber 1988; Flavahan and Vanhoutte 1986). In addition, the heat-induced increase in local metabolic rate increases the oxygen consumption in tissues and decreases the tissue PO_2. A decrease in PO_2 in smooth muscle of blood vessels and in parenchymal cells causes vasodilation and opening of more capillaries. After its initial increase, at a certain tissue temperature and heating time, a decrease in flow is often observed. It may be due to the effects of temperature decrease on certain intracellular or extracellular pathways. It has also been hypothesized that an increase in intravascular pressure within the microcirculation due to increased blood viscosity causes the decrease in flow through the microcirculation. Increase in viscosity is mainly attributed to the increased permeability of vessel walls to plasma (Song, 1984).

In this study, the prostate temperature elevations in response to heating generated by the RF applicator were accompanied by significant increases in prostatic blood flow. The local transient temperature rate may be the dominant factor to trigger the perfusion increase at lower tissue temperatures. Strong correlation between local blood perfusion and tissue temperature was demonstrated when the tissue temperature is higher than 41°C. It implies the dominant roles of local tissue temperature and/or spatial temperature gradient in regulating blood flow. The experimental data can be used to explain different temperature responses observed by previous investigators (Roamer et al. 1985; Xu et al. 1998a). It helps provide a better understanding of the thermoregulation within the canine prostate during transurethral RF hyperthermia. Results of the present study offer an experimental foundation for a more detailed theoretical analysis on the tissue temperature distribution based on the power input and local blood perfusion.

Acknowledgements This research was partially supported by NIH 5 R29 CA67970-03. The authors wish to thank Yuanshui Industrial Company for providing the transurethral thermal therapy system and technical assistance to this research.

References

Baert L, Ameye F, Pike MC, Willemen P, Astrahan MA, Petrovich Z (1992) Transurethral hyperthermia for benign prostatic hyperplasia patients with retention. J Urol 147:1558–1561

Chen C, Xu LX (2002) Tissue temperature oscillations in an isolated pig kidney during surface heating. Ann Biomed Eng 30:1162–1171

Devonec M, Berger N, Fendler JP, Joubert P, Nasser M, Perrin P (1993) Thermoregulation during transurethral microwave thermotherapy: experimental and clinical fundamentals. Eur Urol 23(suppl):63–67

Faber JE (1988) *In situ* analysis of α-adrenoceptors on arteriolar and venular smooth muscle in rat skeletal muscle microcirculation. Circ Res 62:37–50

Flavahan NA, Vanhoutte PM (1986) Effect of cooling on alpha-1 and alpha-2 adrenergic responses in canine saphenous and femoral veins. Pharm Exp Ther 238:139–147

Homma Y, Aso Y (1993) Transurethral microwave thermotherapy for benign prostatic hyperplasia: a 2-year follow-up study. J Endourol 7(3):261–265

Larson TR, Collins JM (1988) Increase prostatic blood flow in response to microwave thermal treatment: preliminary findings in two patients with benign prostatic hyperplasia. Urology 46(4):584–590

Larson TR, Bostwick DG, Corica A (1996) Temperature-correlated histopathologic changes following microwave thermoablation of obstructive tissue in patients with benign prostatic hyperplasia. Urology 47:463–469

Losev ES (1993) Mathematical simulation of thermoregulation in local hyperthermia. Biofizika 38(5):843–848

Marteinsson VT, Due J (1994) Transurethral microwave thermotherapy for uncomplicated benign prostatic hyperplasia Scand. J Urol Nephrol 28:83–89

Martin GT, Haddad MG, Cravalho EG, Bowman HF (1992) Thermal model for the local microwave hyperthermia treatment of benign prostatic hyperplasia. IEEE Trans Biomed Eng 39:836–844

Mulvin D, Creagh T, Kelly D, Smith J, Quinlan D, Fitzpatrick J (1994) Transurethral microwave thermotherapy versus transurethral catheter therapy for benign prostatic hyperplasia. Eur Urology 26:6–9

Nissenkorn I, Meshorer A (1993) Temperature measurements and histology of the canine prostate during transurethral hyperthermia. J Urol 149:1613–1616

Pennes HH (1948) Analysis of tissue and arterial blood temperatures in resting forearm. J Appl Physiol 1:93–122

Ranade GG, Puniyani RR, Huilgol NG (1995) The response of skin microcirculation to hyperthermic stress in tumor patients. Clin Physiol 15:331–337

Roemer RB, Oleson JR, Cetas TC (1985) Oscillatory temperature response to constant power applied to canine muscle. Am J Physiol 249:R153–R158

Rosette JJMCH, de la Froeling FMJA, Debruyne FMJ (1993) Clinical results with microwave thermotherapy of benign prostatic hyperplasia. Eur Urology 23(suppl 1):68–71

Sapozink MD, Stuart DB, Astrahan MA, Jozsef G, Petrovich Z (1993) Transurethral hyperthermia for benign prostatic hyperplasia: preliminary clinical results. J Urol 143:944–950

Sekins KM, Lehmann JF, Esselman P, Dundore D, Emery AF, de Lateur BJ, Nelp WB (1984) Local muscle blood flow and temperature responses to 915 MHz diathermy as simultaneously measured and numerical predicted. Arch Phys Med Rehabil 65:1–7

Song CW (1984) Effect of local hyperthermia on blood flow and microenvironment: a review. Cancer Res 44(suppl):4721s–4730s

Tharp HS, Zhang W (1993) Analytical study of temperature oscillations in living tissues. IEEE Trans Biomed Eng 40:108–110

Vanhoutte PM (1980) Physical factors of regulation. In: Bohr DF, Somly AP, Sparks HV (eds) Handbook of Physiology, Section 2, Circulation, vol 2, Vascular smooth muscle. American Physiological Society, Bethesda, pp 443–474

Wallenstein S, Zucker CL, Fleiss JL (1980) Some statistical methods useful in circulation research. Circ Res 47(1):1–9

Xu LX, Zhu L, Holmes KR (1998a) Thermoregulation in the canine prostate during transurethral microwave hyperthermia, part I: temperature response. Int J Hyperthermia 14:29–37

Xu L X, Zhu L, Holmes K R (1998b) Thermoregulation in the canine prostate during transurethral microwave hyperthermia, part II: blood flow response. Int J Hyperthermia 14:65–73

Zhu L, Xu LX (1999) Evaluation of the effectiveness of during transurethral radio frequency hyperthermia in the canine prostates: temperature distribution analysis. J Biomech Eng 121:584–590

Zhu L, Lemons DE, Weinbaum S (1995) A new approach for predicting the enhancement in the effective conductivity of perfused muscle tissue due to hyperthermia. Ann Biomed Eng 23:1–12